

CONFERENCE PRE-PRINT

DEVELOPMENT AND FUTURE PLAN OF THE NEGATIVE HYDROGEN ION SOURCES FOR NBI AT SWIP

Miao Zhao, Xianming Zhang, Liping Huang, Yuxian Zhang, Weimin Xie, Qi Yu, Yingnan Bu, Guiqing Zou, Shaofei Geng
Southwestern Institute of Physics
Chengdu, China
Email: zhaomiao@swip.ac.cn

Abstract

A radio-frequency negative ion source with an extraction area of $0.32 \times 0.4 \text{ m}^2$ has been developed. It consists of a driver with an inner diameter of 280 mm and a length of 140 mm, coupled with an expansion chamber measuring $500 \times 600 \times 250 \text{ mm}^3$. The magnetic filter field strength is approximately 7 mT. The source operates without the need for a start filament. The design parameters are achieved, though not simultaneously. Building on the development of the single-driver source, a three-driver, three-stage acceleration ion source has been developed and is currently in operation

1. INTRODUCTION

For heating of the large-scale tokamak ITER, the beam energy should be as large as 1 MeV to make sure the beam can be injected into plasma core. The source has to be a negative ion source since the neutralization efficiency of the negative beam can stay above 60 %, when the beam energy reaches 200 keV. And for the advantages of high ionization degree and maintenance-free operation, the RF ion source is chosen as the reference ion source of ITER^[1]. IPP Garching started to develop the negative RF hydrogen ion source in 1998^[2]. The BATMAN, MANITU, RADI, ELISE ion sources have been developed during the past several ten years^[3]. BATMAN and MANITU are single driver sources developed for the study of physical topics such as RF coupling, production of negative hydrogen ions, particle transport mechanism across the magnetic filter field, caesium injection efficiency, beam extraction and acceleration, co-extracted electrons, backstreaming positive ions, etc. RADI and ELISE are half size sources to verify the conception design of multi-driver discharge and size scaling. They are both four driver sources, the difference is that the RADI has no extraction system while ELISE has a three-grid extraction system. The design beam energy of the ELISE is 60 keV, for the limitations of the high voltage power supply. The aiming of this source is to achieve high beam current density (300 A/m^2). This aim has been achieved at the year of 2024^[4].

The physical study of high energy beam acceleration has been undertaken by JAEA and their co-operators. And three-stage acceleration beam source has been successfully developed at JAEA and the beam energy reaches 500 keV^[5]. Conceptual and engineering design of the high voltage negative ion source whose beam energy is as large as 1 MeV has been completed^[6]. Based on these experiences, the full-size sources, SPIDER and MITICA, have been developed at Padova, Italy. Experiments have been carried out on SPIDER and the beam parameters of 50 keV/ $168 \text{ A} \cdot \text{m}^{-2}$ have been reached. Many problems exhibit after the first operation and the source has been shut down temporarily to solve the problems^[7]. The development of full energy source still confronts many problems such as high voltage insulation, faraday shield damage, etc. The accelerator and high voltage bushing of the MITICA source are still under verification, and the test remains unpassed until now^[8]. Also, the transmission line of the ITER NBI is still under construction.

To help to solve some technical problems ITER confronting and to develop the NNBI for CFETR, China has tried to develop a prototype NNBI for the future fusion reactor. A radio frequency negative hydrogen ion source with the designed parameters of 200 keV/20 A/1000s has been developed. It was a multiple driver source.

Firstly, A smaller radio frequency negative hydrogen ion source with an extraction area of $0.32 \times 0.4 \text{ m}^2$ has been developed at SWIP to study the physical and engineering problems. A full solid-state RF generator, providing a total power of 80 kW at a frequency of 2 MHz, is used to generate plasma^[9]. The design parameters for this source are 5 A at 200 kV for 3600 s. Currently, the maximum beam current, beam energy, and beam duration achieved are 13 A, 198 keV, and 5000 s, though these values have not been reached simultaneously. A test stand with the total vacuum chamber volume of 6.5 m^3 and pumping speed of 210000 L/s have been developed. This test stand has two high voltage power supply with parameters of respectively 110 kV/60 A/100s and 200kV/5A/CW, along with an extraction power supply of 10 kV/60 A/5s. Experiments on negative hydrogen ion production, MFF field

optimization, negative ions extraction and acceleration have been carried out. This paper is mainly focused on the source design and primary experimental results of the ion source.

2. SOURCE DESIGN AND TEST STAND

2.1. Beam source

The ion source consists of a driver with an inner diameter of 280 mm and a length of 140 mm, along with an expansion chamber with the dimensions of $500 \times 600 \times 250 \text{ mm}^3$. The driver mainly contains the backplate, the quartz cylinder, the antenna, the faraday shield, a special designed cooling water backplate, and a plate to install the cusp field magnets. The water inlets and outlets for the faraday shield and the special backplate are positioned on the driver backplate. Three circular shaped magnets arrays are inside the magnets plate with the polar of the two adjacent magnets in the opposite direction and the distance between the center of them is 50 mm. The distance of these magnets to the plasma is 15 mm (thickness of the faraday shield backplate). There are other four ports on the driver backplate, and now one of them is used as gas fed in port.

The antenna consists of a four-turn coil, a framework made of Teflon, and the outer perimeter of the coil is surrounded by soft iron material. A Faraday screening made of molybdenum coated copper is installed inside the quartz vessel to prevent damage of the quartz from plasma etching. The faraday shield has water channels at the lateral wall to withstand heat load of about 40 kW. And a special plate is put inside the back side of the driver to withstand the heat load of the back streaming positive ions produced in the accelerator when the negative ions collide with the neutral particles in the acceleration gap.

The expansion chamber is made of 316L stainless steel. There are water channels in the lateral wall and backplate of it, and a special water channel is near the connection part of the chamber and the driver to prevent the sealing O-ring there from damage. There are cusp field magnets in the backplate and lateral wall, and the distance of them to the inner wall of the chamber is 6 mm. The magnets on the lateral wall are in a modular component and can be easily removed from the source. The magnetic filtering field is generated by an array of 10 magnets, each with dimensions of $90 \text{ mm} \times 50 \text{ mm} \times 20 \text{ mm}$. And the gap distance between two adjacent magnets is 40.5 mm. They are installed in a movable frame structure with soft iron surrounding the magnets, and other parts to fix the magnets are made of aluminium. It produces a magnetic field with the strength of 7 mT near the plasma grid. There are other four ports on the chamber backplate, and one of them is used to measure the pressure by a thin film gauge. The other two of them are for caesium guns, as shown in the figure 1.

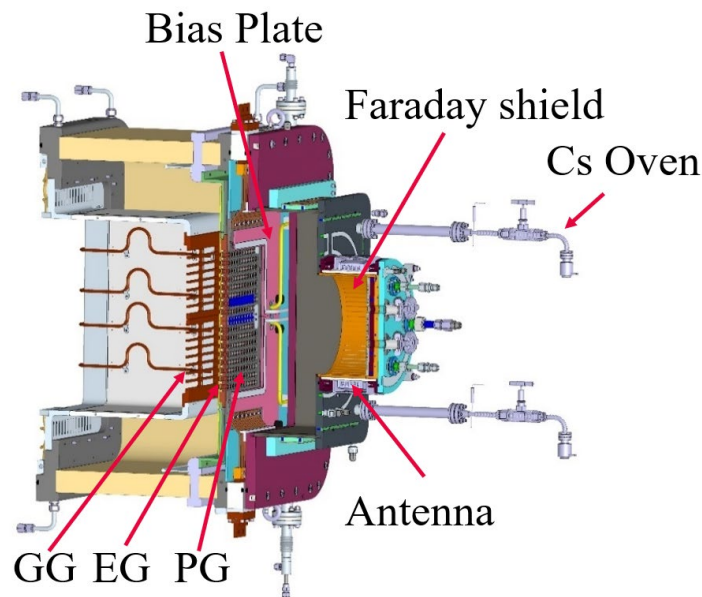


FIG. 1. Ion source.

An alternative way to produce the magnetic filter field is by a large current flowing through the PG, and current ports have always been designed to realise it. A current distributor is developed to make the current density on the PG almost uniformly. Also, the current return feeder made of two copper bars have been designed.

Pressure controlled gas feeding technique has been developed that the plasma can be generated without a start filament. The plasma can be directly ignited at the pressure of larger than 0.3 pa, and for pressure lower than that the plasma can be ignited at a higher pressure and then lower down to the destination pressure.

The extraction system (the accelerator) consists of three grids: the plasma grid, the extraction grid, and the ground grid. The maximum voltage can be applied on the extraction gap is 10 kV, while the maximum voltage on the acceleration gap is 200 kV. The extraction area is 0.0409 m², consisting of 266 holes with a diameter of 14 mm each. There is a bias plate before the PG. And the distance between the PG and the BP is 10 mm. the material of the PG is molybdenum, and the material of the EG and GG is copper. The thickness of the three grids are respectively 6 mm, 15 mm and 10 mm. The distances of the extraction and acceleration gaps are respectively 5 mm and 88 mm. The material of the insulation between the grid supporters is epoxy.

Three-dimensional fluid models have been developed to study the effects of the gas pressure, the configuration of the magnetic filter field, the effect of the Faraday shield on the electron density, electron temperature and negative hydrogen ion distributions. [10-13] According to the simulation results, a soft iron magnetic shielding layer, approximately 6 mm thick, was added to the backplate of the ion source expansion chamber. This magnetic shielding layer, together with the filtering magnetic field and the confinement cusp-field, forms the magnetic field configuration of the ion source.

2.2. Test stand I

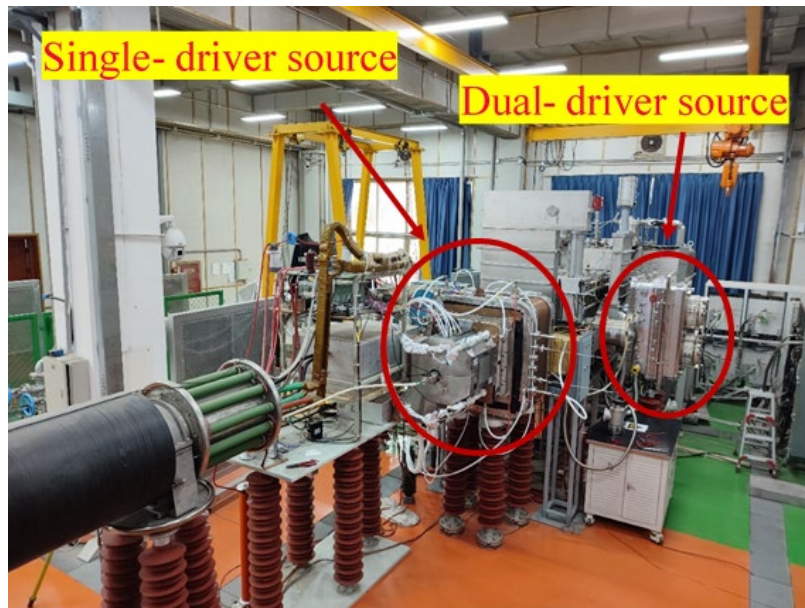


FIG. 2. Test stand I.

Test stand I is shown in Fig.2. And it is designed for testing the single-driver ion source mentioned above and the dual-driver source. The dual-driver source has no extraction system and is designed to verify the conception of multi-driver discharge. The plasma will be generated by the independent discharge of the two drivers. At the moment, the stand owes only one RF power supply of 2 MHz, 80 kW. The extraction power supply is on the high voltage platform and its parameters are 10 kV, 60 A respectively. The isolation transformer of this stand is 200 kV. The RF power supply, the PG bias power supply, the PG current power supply, the control units of gas feeding system, caesium feeding system are on the high voltage platform. Deionized water with resistivity of about 2M $\Omega \cdot \text{cm}$ is injected into the parts needing cooling on the high voltage potential. The vacuum system mainly contains

two cube chambers with total volume of 6.5 m^3 , five cryopumps with total pumping speed of $210000 \text{ L}^3/\text{s}$, several turbo molecular pumps, roots pumps and machinery pumps as fore pumps. A port is just left behind the expansion chamber to pump the source firstly for vacuum gauge validation. And a quadrupole mass spectroscopy is installed at the main chamber to measure the pressures of the gas impurities in the chamber, especially the water pressure which is very important for the caesium injection. Also, the PG temperature control system is developed, and fluorinated liquid is used to raise the temperature of the PG to up to $100\sim 250 \text{ }^\circ\text{C}$.

2.3. Diagnostics

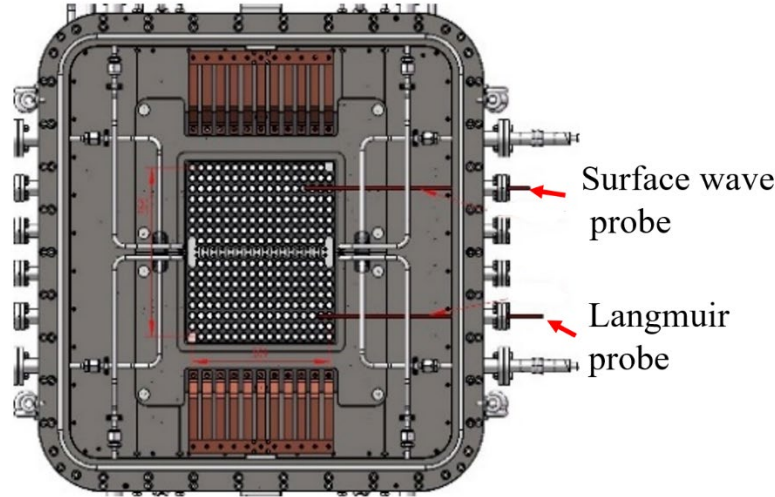


FIG. 3. Layout of the diagnostic ports

A diagnostic flange made of polytetrafluoroethylene (PTFE) is placed before the PG. Besides the ports left for the water inlets and outlets of the PG and BP and the current port for the PG, there are four ports left for diagnostics in each side of the flange. Moveable Langmuir probes and surface waves probes are used to measure the electron density and temperature. OES of Cs 852 nm is used to measure the caesium line density. Cavity ring down method is used to measure the H^- density, it hasn't been used at the moment for the reason that the channel of the light is shielded by some ceramic nuts.

There are no beam line components on the vacuum chamber, such as neutraliser, residual ion deflector and calorimeter. The extraction and acceleration beam currents and voltages are measured by hall sensors and voltage dividers. There are two targets on the platform, one is a tungsten filament and molybdenum target 1 m downstream the GG, the target is moveable and the temperature distribution by infrared cameras placed at the top of the vacuum chamber. The other one is a backplate 5 m downstream the GG and the temperature distribution is also measured by infrared camera. Experimental results on the beam profile measurements and divergence study will be reported in the future and are not included in this paper.

3. EXPERIMENTAL RESULTS

3.1. Plasma parameters

The electron density and temperature distributions of the plasma before the PG are measured by movable static probes. Experiments on the effects of the above-mentioned source parameters on the plasma parameters are conducted to verify the simulation model^[14].

Figure 4 shows the electron density and temperature distribution measured by Langmuir probes. At the moment, the probes are moved by hand so it can't be moved very fast, so the experiments are carried out under low RF power of 5 kW and pressure of 0.5 Pa. And it was without caesium feeding. The electron density is about $5\sim 6 \times 10^{16} \text{ m}^{-3}$ and the plasma density homogeneity is 90 %.

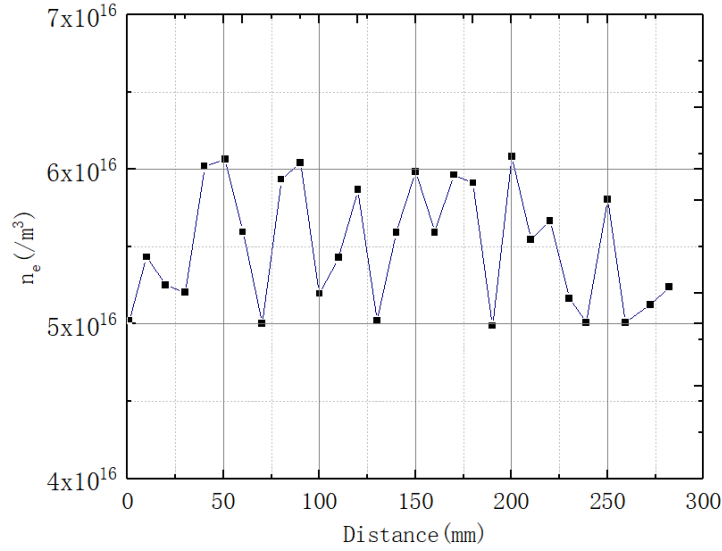


FIG. 4. Plasma density distribution before the PG at RF power of 5 kW and pressure of 0.5 Pa

3.2. Beam extraction

Currently, at an RF power of 35 kW, the extracted negative hydrogen beam parameters are 13 A at 100 keV for 0.1 s, with a corresponding beam current density of 317 A/m². For long-pulse operation, the beam parameters are 50 keV at 0.25 A for 5000 s. For high beam energy operation, the parameters are 198 keV at 0.15 A for 3 s. The design parameters have not yet been achieved simultaneously due to limitations in the ion source test stand, which currently lacks a dedicated calorimeter. As a result, the beam energy impacting the back plate of the vacuum chamber must be kept within limits, and the electrode transparency is too high to withstand long-pulse, high-power beams simultaneously. Additionally, the ratio of electrons to negative hydrogen ions remains below 1. Some typical waveforms are shown in Fig. 5. Figure 5(a) shows a stack graph of beam extraction at RF power of 5 kW and pressure of 0.5 pa at different extraction and acceleration voltage, the extraction current increase from 3 A to 6 A, while the acceleration current increases from 1.2 A to 2.3 A. The acceleration voltage remains unchanged, this shows increasing the extraction current can enhance the extracted negative hydrogen ions. Figure 5(b) shows the high energy extraction, the extraction voltage and the acceleration voltage are 2 kV and 196 kV, respectively. It's without caesium. The extraction current is 0.5 A and the acceleration current is 0.2 A. The pulse duration is 1 s. Figure 5(c) shows that at a pressure of 0.7 pa and RF power of 35 kW, and the extraction voltage and the acceleration voltage of 9 kV and 75 kV, and with the caesium injected into the source, the extraction current is 22 A and acceleration current is 13 A. The electron to ion ratio is lower than 1. Since the beam directly hit on the backplate, the beam power and pulse duration are limited on this campaign of experiments. Figure 5(d) shows the waveform of the long pulse extraction, at an RF power of 5 kW, extraction and acceleration voltage of respectively 2 kV and 50 kV, 0.3 A negative ion beam has been stably extracted for as long as 5000 s.

The statistical diagram of the beam current before and after the caesium injection is shown in figure 6, and the results show that the current increases after the caesium injection. It usually takes several days for the cesium covered on the plasma grid to get into a good condition for high beam current extraction. Figure 7 shows the relationship between the total extraction current and the H⁻ beam current versus the RF power, both the two currents increase with the RF power, and the electron to ion ratio is about 1. These experiments are conducted under the condition of caesium injection.

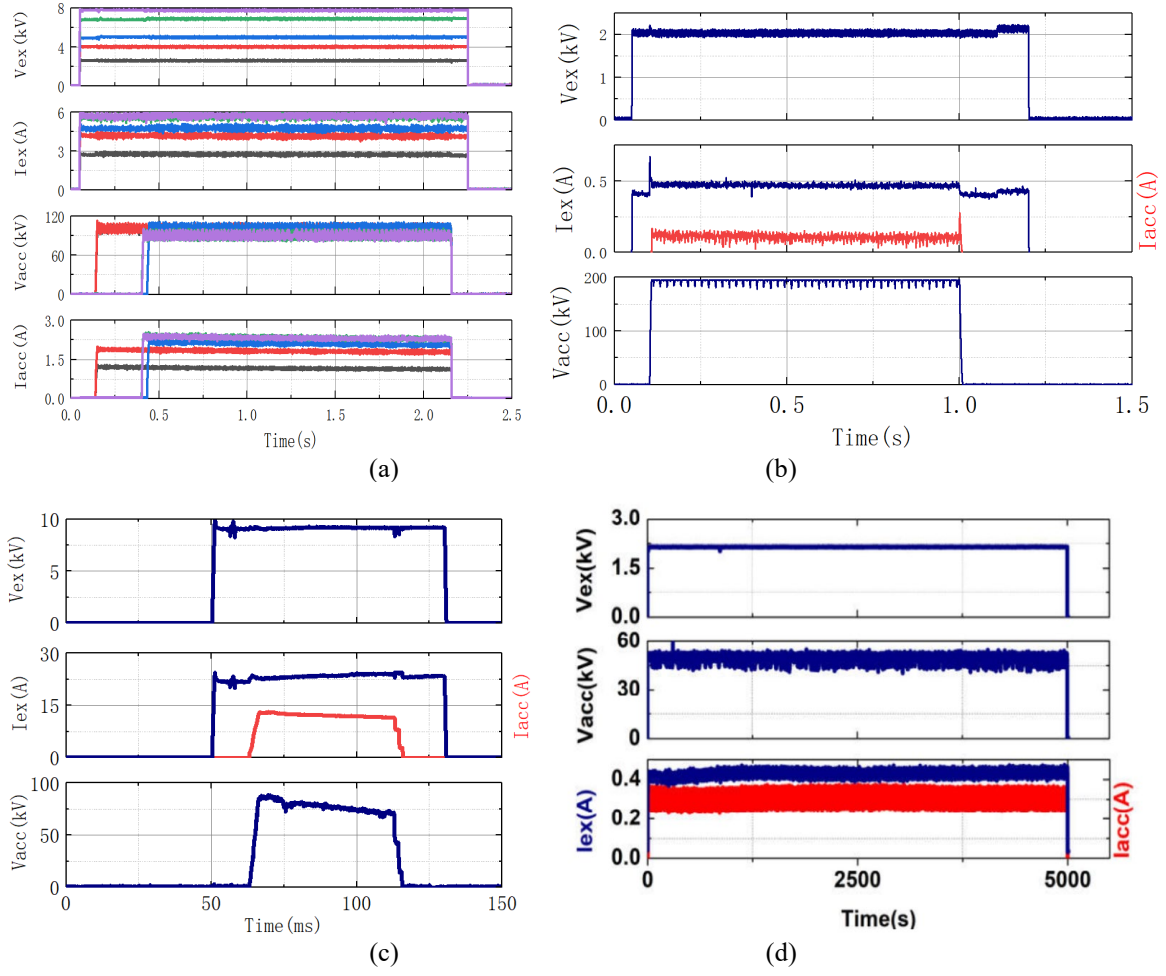


FIG. 5. Typical Waveforms of the extraction current, extraction voltage, acceleration current and acceleration voltage (a) stack graph, (b) high beam energy extraction, (c) large beam current extraction, (d) long pulse extraction

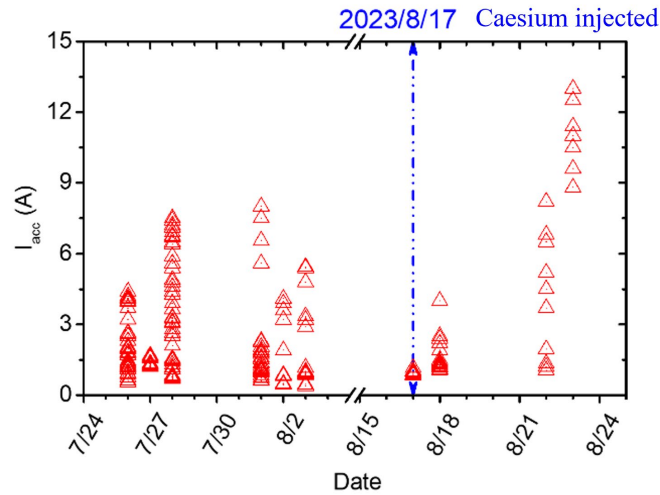


FIG. 6. Statistical diagram of the extracted H^- current

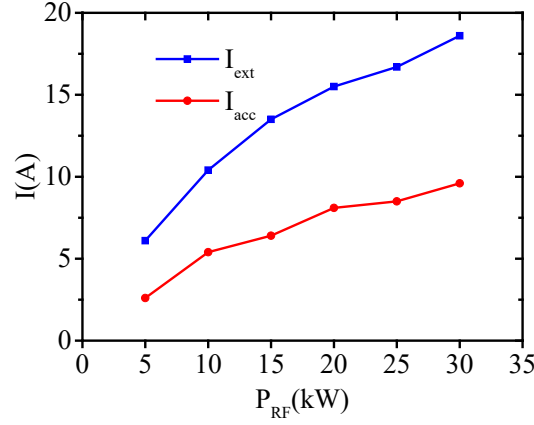


FIG. 7. Extraction and acceleration current versus RF power

4. FUTURE PLAN

Furthermore, another ion source with three drivers, an extraction area of $0.32 \times 1.2 \text{ m}^2$, and a three-stage acceleration system has been developed and tested on a bigger stand. The test stand II is shown in Fig. 8. The test stand owes the needed beam line components, such as neutralizer, a magnetic residual ion deflector, a calorimeter. The vacuum chamber mainly contains two cylinders of the volume of 36.3 m^3 and a connection part of the volume of 12.7 m^3 . The first tank is called the source tank for installation of ion source. The connection part has the neutralizer inside. The second tank is the beam components tank, and it contains magnetic residual ion deflector and calorimeter. Each of the tank will be equipped with two panel cryopumps, of which the pumping speed is 1000000 L/s . With a such structure, the pressure in the accelerator and the neutralizer can be controlled independently, i.e. maintaining a relatively low pressure of the order of 10^{-3} Pa in the accelerator and by secondary gas injection a relatively high pressure of 10^{-2} Pa in the neutralizer. The requirements of both less stripped loss of negative ions in the accelerator and thick enough target in the neutralizer have been thus satisfied.

The test stand for this source is larger and includes a calorimeter capable of withstanding high-power beam energies. The design parameters for this source are 300 A/m^2 at 500 keV for 100 s . Although at the first stage, the acceleration power supply is $200 \text{ kV}/20 \text{ A}$, the transformer has been developed at an isolating voltage of 600 kV for future upgrade. And at the first stage, only the beam tank is ready and the ion source is installed on the tank directly for early study, and the four panel cryopumps are still under test so the vacuum is maintained by two commercial cryopumps installed on the lateral flange of the cylinder, the pumping speed at present stage is 20000 L/s . Thus $2/3$ of the plasma grid is covered to obtain an acceptable pressure gratitude to ensure the pressure in the extraction and acceleration gap is low enough to be avoided to suffer from high voltage breakdown.

The first plasma has been successfully generated, and a small beam current of approximately 0.4 A has been extracted, with a pulse length of 100 s .

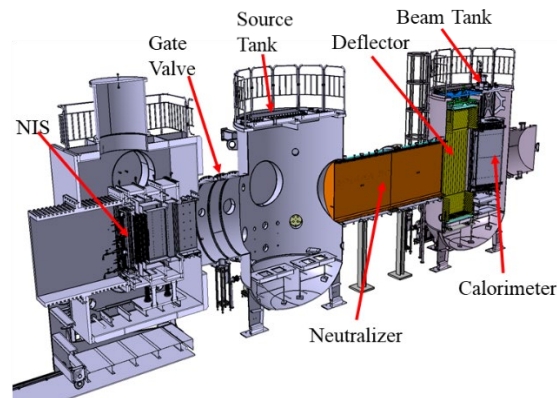


FIG. 8. Test stand II

5. SUMMARY

A radio-frequency negative ion source with an extraction area of $0.32 \times 0.4 \text{ m}^2$ has been developed. It consists of a driver with an inner diameter of 280 mm and a length of 140 mm, coupled with an expansion chamber measuring $500 \times 600 \times 250 \text{ mm}^3$. The magnetic filter field strength is approximately 7 mT. The source operates without the need for a start filament and the plasma can be directly excited by the RF field produced by the antenna at a pressure of 0.3-1 Pa. At the moment, the maximum parameters of 198 kV/13A/5000s have been arrived. The parameters are not reached simultaneously, due to the lack of calorimeter on test stand and the current limitations of the high voltage power supply. The plasma homogeneity is 90 %, which meets the ITER requirements. Building on the development of the single-driver source, a three-driver, three-stage acceleration ion source has been developed and is currently in operation. A larger scale test stand is developed for this source, and the test stand has all the required beam line components for beam transport and neutralization study.

ACKNOWLEDGEMENTS

This work was supported by the National Key R&D Program of China (No. 2017YFE0300102) and the National Natural Science Foundation of China (No. 11905048).

REFERENCES

- [1] HEMSWORTH R, DECAMPS H, GRACEFFA J, et al. Status of the ITER heating neutral beam system [J]. 2009, 49(4): 045006.
- [2] FRANK P, FEIST J H, KRAUS W, et al. A large-area RF source for negative hydrogen ions, F, 1998 [C].
- [3] HEINEMANN B, FANTZ U, KRAUS W, et al. Towards large and powerful radio frequency driven negative ion sources for fusion [J]. 2017, 19(1): 015001.
- [4] WÜNDERLICH D, RIEDL R, FRÖSCHLE M, et al. ITER-relevant 600 s steady-state extraction of negative hydrogen ions at the test facility ELISE [J]. 2024, 65(1): 014001.
- [5] KASHIWAGI M, HIRATSUKA J, ICHIKAWA M, et al. 100 s negative ion accelerations for the JT-60SA negative-ion-based neutral beam injector [J]. Nuclear Fusion, 2022, 62(2): 026025.
- [6] DE ESCH H, KASHIWAGI M, TANIGUCHI M, et al. Physics design of the HNB accelerator for ITER [J]. 2015, 55(9): 096001.
- [7] PAVEI M, GASPARRINI C, BERTON G, et al. Status of SPIDER beam source after the first 3.5 years of operation [J]. Fusion Engineering and Design, 2023, 192: 113831.
- [8] PATTON T, CHITARIN G, PILAN N, et al. Progress and results of the first high voltage vacuum insulation tests in MITICA [J]. Fusion Engineering and Design, 2025, 220: 115349.
- [9] LEI G J, YAN L W, LIU D P, et al. Development of megawatt radiofrequency ion source for the neutral beam injector on HL-2A tokamak [J]. Nuclear Fusion, 2021, 61(3): 036019.
- [10] Yingjie Wang, Jiawei Huang, Yuru Zhang, et al. Influence of magnetic filter field on the radio-frequency negative hydrogen ion source of neutral beam injector for China Fusion Engineering Test Reactor [J]. Plasma Science and Technology, 2021, 23(11): 8.
- [11] XING S. 3D fluid model analysis on the generation of negative hydrogen ion for CFETR NBI [J]. Plasma Science & Technology, 2023.
- [12] CHEN C, WANG Q, ZHAI W, et al. Three-dimensional modeling of the large and powerful radio frequency negative hydrogen ion source with Faraday shield [J]. Fusion Engineering and Design, 2024, 204: 114526.
- [13] CHEN C, ZHAI W, WANG Q, et al. Investigation on the spatial distribution of H⁻ ions in RF ICP source with Faraday shield [J]. 2024, 67(1): 015025.
- [14] XING S-Y, GAO F, ZHANG Y-R, et al. 3D modeling of a double-driver ion source considering ion magnetization: an investigation of plasma symmetry modulation methods [J]. Nuclear Fusion, 2024, 64(5): 056015.